Comparison Between Wear Resistance of Functionally Graded And Homogenous Al-SiC Nanocomposite Produced by Friction Stir Processing (FSP)

M. Saadatmand and J. Aghazadeh Mohandesi

In the present work, wear resistance of a homogeneous and functionally graded Al/SiC nanocomposite produced by friction stir processing was studied. According to the wear test results, the friction coefficient of the functionally graded nanocomposite was slightly less than that of the homogeneous nanocomposite (i.e., 0.7 compared to 0.8); this may be due to higher surface hardness of the functionally graded composite. In both cases, the weight loss increased with increasing applied loads; however, weight loss for the functionally graded nanocomposite was lesser under each applied load. Regarding surface studies by Scanning Electron Microscope (SEM) and Optical Microscope (OM), the functionally graded nanocomposite showed less micro-galling and other surface damages; this can be attributed to its surface hardness and high work of fracture.

1. Introduction

The functionally graded material (FGM) as composite may contain reinforcement particles whose volume fraction varies continuously, thereby providing a variable microstructure with continuously changing properties. This type of FGM is useful in applications where a combination of high surface wear resistance and high work of fracture of the interior bulk material is required. This balance of properties may not be achievable in many cases in monolithic or homogeneous materials (Ref 1).

Aluminum alloys are in widespread demand in the automotive, aviation, and military industries due to their lightness, durability, stiffness, preferable corrosion properties, and capability of augmentable endurance via aging (Ref 2). Aluminum alloys are preferred as matrix materials for metal matrix composites due to their ductility and hardness combinations, enhanced endurance, and rigidity (Ref 3-5). SiC nanoparticles are the preferred strengthener because they possesses high hardness and wear strength capabilities (Ref 3, 5, 6).

There are many ways to produce FGMs, including centrifugal casting, powder metallurgy (PM), thermal spray, and spark plasma sintering. For Metal Matrix Nano Composites (MMNCs) prepared by the liquid metallurgy route, the nanoparticles tend to agglomerate into coarse clusters and it is hard to avoid the interfacial reaction between the reinforcement and metal matrix and the formation of some detrimental phases. In the PM technique consisting of conventional pressing and sintering, the

mixing of nanosized ceramic particles is lengthy, expensive, and energy consuming. Also, the nanosized reinforcements always prevent composites from densification.

The FSP technique [Fig. 1 (Ref 7)] has been used for producing Mg- (Ref 8) and Al-based nanocomposites (Ref 9-11). In contrast to PM and liquid metallurgy, FSP provides the following advantages: (1) a solid state process to prevent problems associated with liquid metallurgy; (2) severe plastic deformation to promote mixing and refining of constituent phases in the material; and (3) hot consolidation to form fully dense solid. During this process, the material undergoes intense plastic deformation, which may result in significant homogenized nanoparticle distribution (Ref 12).

Materials used for tribological applications should be able to support a load without distortion, deformation, or fracture, and should have low wear almost always combined with low friction coefficient under sliding contact (Ref 13). The friction and wear behavior of the composites is known to be dependent on the microstructural characteristics of the matrix and also on the type, shape, size, and volume fraction of the reinforcing particles (Ref 13).

A high number of studies are reported in the literature regarding the tribological behavior of homogeneous metal matrix composites (Ref 14-16); however, the information about the tribological response of these materials when prepared as a functionally graded (FG) composite using FSP is scarce. Therefore, the study of wear resistance of an aluminum-based FG composite produced employing FSP may be of research interest. The aim of the present work was to investigate the wear resistance of an aluminum-based FG composite and its plausible advantage compared with homogeneous Al-SiC composite.

2. Experimental Procedures

Aluminum 6061-T6 rolled plates (330 mm × 50 mm × 8 mm) with chemical analysis [(wt.%): 0.54 Si, 0.8 Mg, 0.07 Mn, 0.2 Cu, 0.4 Fe, and Al (balance)] and nanosized SiC powder

M. Saadatmand and **J. Aghazadeh Mohandesi,** Department of Mining and Metallurgical Engineering, Amir Kabir University of Technology, Hafez Ave, Tehran, Iran. Contact e-mail: agazad@aut.ac.ir.
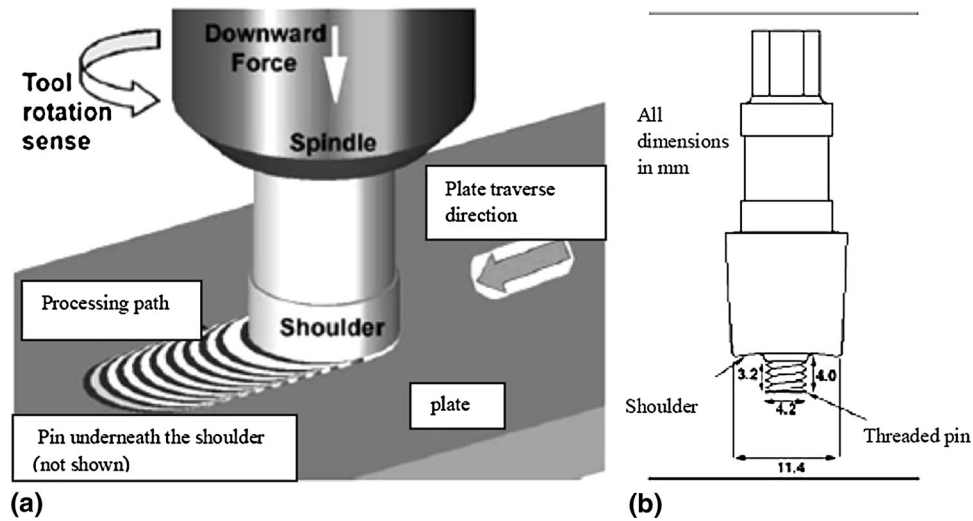
Fig. 1 Schematic illustration of (a) friction stir processing and (b) the tool used in the present investigation (Ref 7)

Fig. 2 Upper surface of groove cut on the FSPed zone

(purity: 99.5% and nominal diameter: 50 nm) were used as the base material and reinforcement particle, respectively.

Two types of tools made of steel H-13 were used, with shoulder diameter of 20 mm, threaded pin diameter of 7.8 mm, one with a pin length of 6 mm (A), and the other with 3.2 mm (B). The difference between the homogeneous and FG composite is in the shape of the pin.

The tool rotation speed was set at 1600 rpm and its advancing speed at 40 mm/min. The tool axis was tilted by 3° with respect to the vertical axis of the plate surface. According to the previous work published (Ref 17), to optimize the homogeneity of particles inside the stir zone, the above-mentioned conditions were chosen. To produce the FG composite, SiC particles were packed into a groove of 5.9 mm in depth and 3 mm in width ground on the samples. Consequently, the specimen was subjected to four FSP passes using tool A in order to improve the homogeneity of the particles. Then, to induce a volume fraction gradient of nanosized SiC across the thickness of the plate, again a groove of 2 mm in depth and 5 mm in width was made in a straight line along the middle of composite zone, as shown in Fig. 2; similarly, the process was performed using tool B.

For comparison, the homogeneous composite with the same volume fraction of the surface layer of the FG composite (i.e., 16% as it will be discussed later in this paper) was fabricated. To produce the homogeneous composite, SiC particles were packed into a groove of 5.9 mm in depth and 5 mm in width ground on samples. Quantitative assessment of SiC particulates was carried out on the FG samples using Energy-Dispersive Spectroscopy (EDS) line scan analysis of the Si component. Line scans were performed on the midline of the cross section
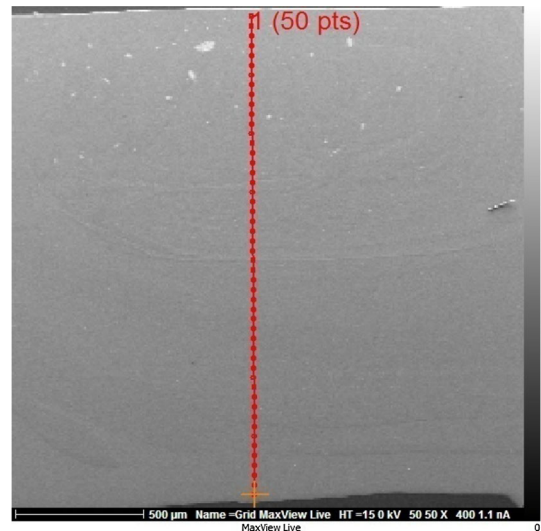

Fig. 3 Positions in the central area of a transverse section for the EDS line scan and hardness test

from the top to the bottom of the samples and measured along three parallel lines separated by a distance of 0.5 mm (Fig. 3). The interval between the points on each line was 350 μm.

The microhardness profile was measured with Vickers microhardness tester at 100 g load and a dwell time of 10 s. Microhardness was performed on the midline of the cross section from the top to the bottom of the samples and measured along three parallel lines separated by a distance of 0.5 mm and an interval between the points on each line of 350 μm. A room

temperature tensile test was carried out using an Instron servo hydraulic machine at a strain rate of 5×10^{-3} s^{-1}, according to the ASTM standard. Figure 4 shows the position and dimensions of the tensile specimen. Samples were cut perpendicular to the FSP direction and prepared by standard metallographic procedures. Microstructural characterizations were conducted in both the etched and unetched conditions using Optical Microscopy (OM). The etchant used was Keller's reagent (150
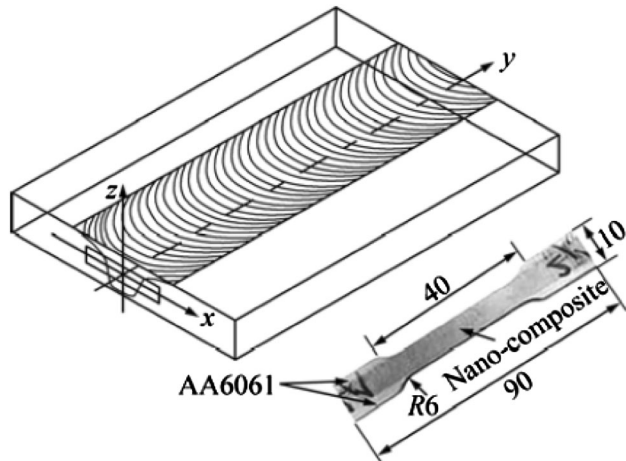
mL water, 3 mL nitric acid, 6 mL hydrochloric acid, and 6 mL hydrofluoric acid).

Wear experiments were conducted at room temperature under constant loads of 10, 20, and 30 N and a sliding velocity of 0.1 m/s, in a pin-on-disk tribometer, without lubrication. The counterpart pin was made of AISI GCr15 steel with a hardness value of 60 HRC. Before the wear test, the surface of the disks was ground by 1000 grit abrasive paper. The disk was cleaned in acetone and weighed prior to testing. The friction coefficient between the pin and disk was determined by measuring the frictional force with a stress sensor. The experiments were stopped at the end of 1-km running to measure the weight loss. Also, the morphological studies of the worn surfaces were made by SEM.

Fig. 4 Position and dimensions of tensile specimen according to ASTM E8 (all dimensions are in mm)

3. Results

3.1 Surface Microstructure

Macroscopic appearance of nugget zone of the FG and homogeneous composite is shown in Fig. 5. There are no voids and cracks in the cross section of both samples. As indicated in Fig. 5(b), the area with dark color shows the area with higher volume fraction of SiC particles. Some agglomerated particles are observed in the Fig. 5(a). Figure 6 indicates an optical micrograph of the FG and homogeneous composite surface.

Considering Fig. 6, it is relatively clear that the grain size in the surface of the FG composite is less than that of the
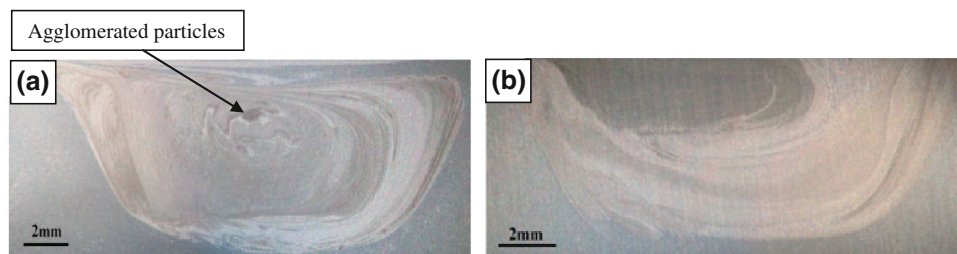

Fig. 5 Optical macroscopic appearances of cross sections: (a) homogeneous and (b) FG composite
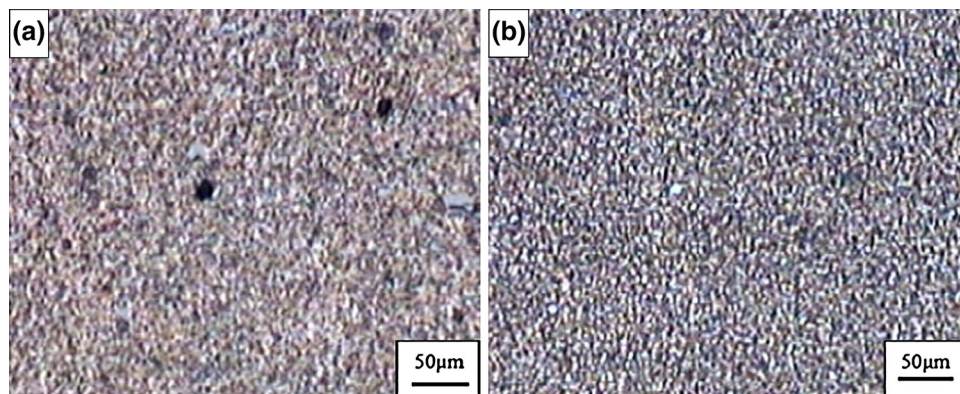

Fig. 6 Optical micrograph of stirred zone in homogeneous (a) and FG (b) composite after four passes FSP

homogeneous composite. The stirred zone (SZ) is characterized by equiaxed and fine grains due to the severe plastic deformation and frictional heating, leading to recrystallization in the SZ. Formation of fine grains in the aluminum alloys during FSP is attributed to different restoration mechanisms such as dynamic recovery (DRV), geometric dynamic recrystallization, and discontinuous dynamic recrystallization (DDRX).
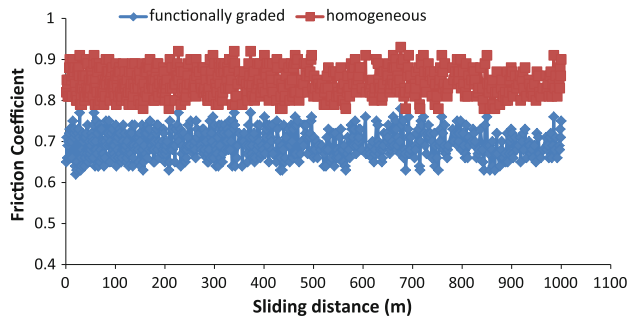

Fig. 7 The friction coefficient of the homogeneous and FG composite as a function of sliding distance at an applied load of 30 N
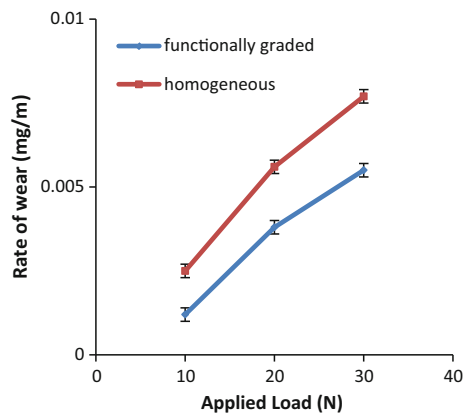

Fig. 8 The rate of wear as a function of applied load for the FG and homogeneous composite

The surface hardness of the nugget in the homogeneous composite was about 140 HV, slightly less than that of the FG composite surface (i.e., about 155 HV); it seems that this discrepancy is due to performing FSP two times on the surface of the FG composite to induce a FG nanoparticle distribution, resulting in finer grains and less clustering areas of SiC particles on the surface of the FG composite (Ref 11).

3.2 Wear Test

Figure 7 shows the friction coefficient of the homogeneous and FG composite as a function of sliding distance at an applied load of 30 N.

As depicted in Fig. 7, the values of the friction coefficient for the homogeneous and FG composite are at an average ~ 0.8 and ~ 0.7, respectively. The lesser friction coefficient of the FG composite could be attributed to higher hardness of the FG composite surface compared with the homogeneous composite surface; this is in agreement with results obtained by Gomes (Ref 13). Since the shear stress is due to the friction force between the two surfaces, the lesser the friction coefficient, the lower the shear stress developed, and consequently the weight loss decreases. So, we expect lower weight loss for the FG composite.

Figure 8 shows the variation of wear rate of the FG and homogeneous composite as a function of applied load. Evidently, the wear rate of the FG composite is less than that of the homogeneous composite irrespective of all applied loads, and for both composites wear rate increased with increasing load.

3.3 Worn Surface Observations

Figure 9 shows the worn surface of the homogeneous composite, tested at a sliding distance of 1 km under 30 N load, imaged in the Secondary Electron (SE) mode.

The worn surface morphology of the homogeneous composite is characterized by the existence of large cavities and micro-galling which show extensive plastic deformation. Also, abrasion grooves formed parallel to the sliding direction were relatively deep.

Figure 10 shows the worn surface of the FG composite, tested at a sliding distance of 1 km under 30 N load, also imaged in the SE mode.
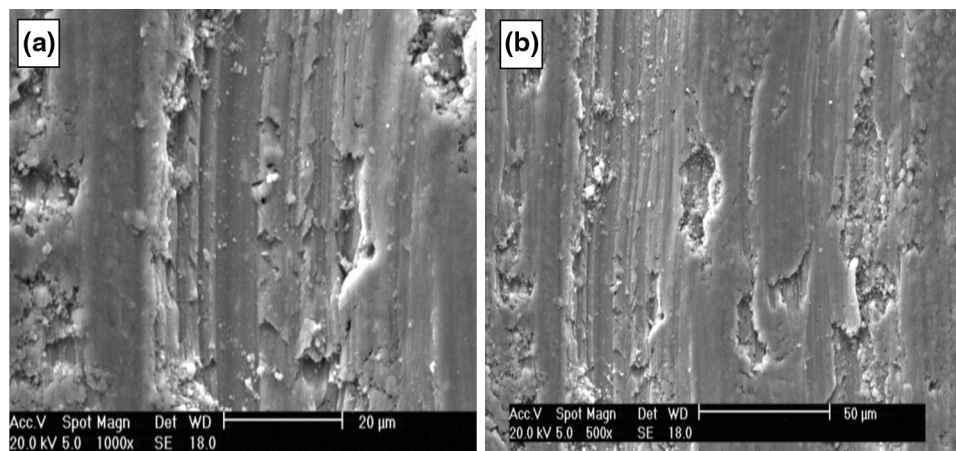

Fig. 9 Worn-out surfaces of the homogeneous composite under load of 30 N
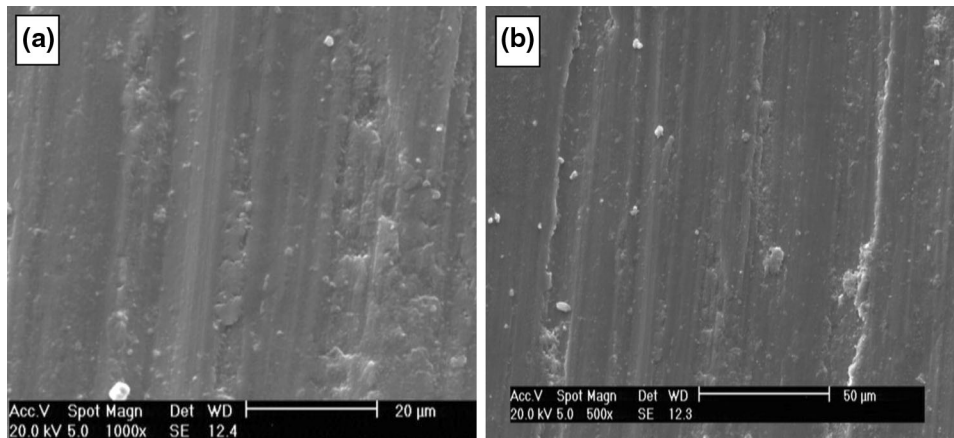
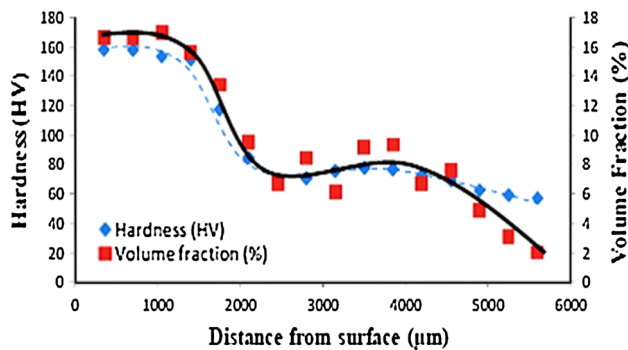**Fig. 10** Worn-out surfaces of the FG composite under load of 30 N

Fig. 11 Microhardness and volume fraction of SiC (%) as a function of distance from the surface of the FG composite

Abrasion grooves and damaged areas (pits) were observed parallel to the sliding direction. The size and amount of grooves and micro-galling were found to be significantly lesser for the FG composite.

Figure 11 indicates the profile of microhardness and volume fraction of SiC (%) as a function of distance from the surface of the FG composite.

As shown in Fig. 11, the volume fraction of SiC (%) on the surface is about 16% and decreases continuously with distance from the surface, and as anticipated the microhardness value follows the same pattern of the volume fraction of SiC.

Figure 12 indicates the EDS analysis of the composite zone (nugget) for the homogeneous composite after performing four passes of FSP. According to the quantitative assessment of SiC particulates, the volume fraction of SiC (%) was about 16%, similar to the surface volume fraction of the FG composite.

Although there is a similar SiC volume fraction on the surface of both composites, regarding the worn surface studies, it seems that resistance to micro-galling for the FG composite is more than that of the homogeneous composite. Apart from higher microhardness for the FG composite surface, the work of fracture can also affect the resistance to micro-galling (Ref 18-20).

Figure 13 illustrates the stress-strain diagram of the homogeneous and FG composite. The step-like stress drop in the stress-strain diagram of the FG composite is due to fracture of the FG layers (Ref 21, 22).

Since the area under the curve is greater for the FG composite, it could be concluded that the work of the fracture of the FG composite is more than that of the homogeneous composite. The mechanical properties of the FG composite are superior to that of the homogeneous composite having a SiC content corresponding to the high SiC region (i.e., surface of FG composite) (Ref 23). For the FG composite, subsurface layers with lower SiC volume fraction absorb more energy, leading to an increased level of work of fracture, compared with the homogeneous composite (Ref 23). Moreover, as shown in Fig. 5(a), the cluster formation of the reinforcement particles decreases mechanical behavior. Also, regarding research carried out by Lin (Ref 23), improvement in the work of fracture of the FG composite may be due to (i) simple retardation of the crack when it reaches the interlayer boundary; (ii) the presence of the some layers changing the geometry and/or size of the plastic zone from the start of loading, thus affecting the propagation of the crack; (iii) a reduction in stress intensity factor K at the crack tip due to the differences in properties between the layers.

In general, the asperities, i.e., roughness surface, play a vital role during the wear process (Ref 24). When two surfaces come into contact, initially, they only touch at a few of these asperity points. These asperities cover only a very small portion of the surface area. As a result, very high stresses will be developed in these small surface areas, where wear originates at these points; thus, having insight into its behavior is essential when studying materials in contact. From Fig. 9 and 10, it is clear that the micro-galling amount is less for the FG composite than for the homogeneous composite. Therefore, it could be concluded that the surface asperities of the FG composite, because of higher work of fracture, have higher resistance to fracture. In addition, because of higher work of fracture, the produced groove depth on the surface of the FG composite is less than that of the homogeneous composite.
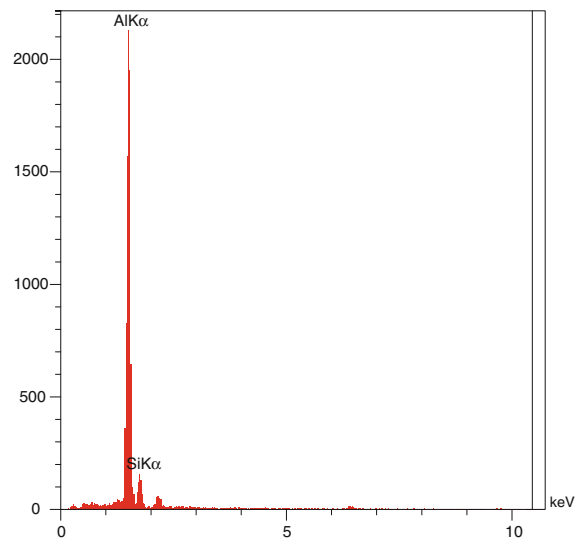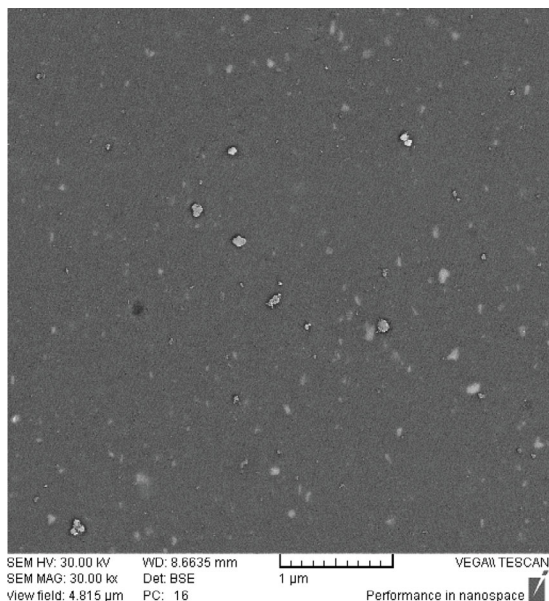
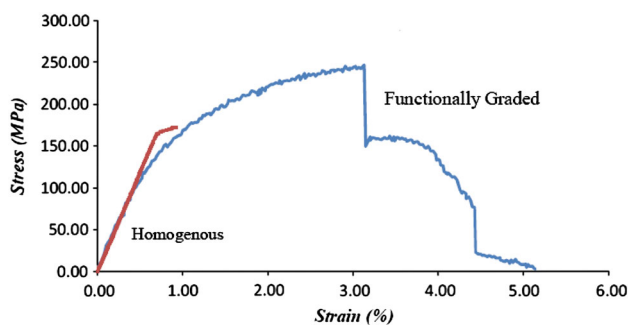**Fig. 12** EDS analysis of homogeneous composite zone

Fig. 13 Stress-strain diagram for homogeneous and FG composite

4. Conclusions

In this work, we successfully produced a FG composite with high wear resistance and work of fracture compared with a homogeneous composite.

– The friction coefficient of the FG composite was less than that of the homogeneous composite. It could be due to higher surface hardness of the FG composite. As a result, the weight loss for the FG composite was lesser under each applied load.
– The FG composite showed higher work of fracture than the homogeneous composite. It could be attributed to the FG structure of the FG composite. On the other hand, micro-galling depends on the work of fracture. Therefore, the micro-galling amount was lesser on the FG composite surface.

References

1. S. Nai, M. G, and C. Lim, Synthesis and Wear Al Based Functionally Graded Composite, *Mater. Sci. Technol.*, 2004, **20**, p 57–67
2. Y. Sahin, Wear Behaviour of Aluminium Alloy and Its Composites Reinforced by SiC Particles Using Statistical Analysis, *Mater. Des.*, 2003, **24**, p 95–103
3. B. Dikici, M. G, and C. Tekmen, Corrosion Behavior of an Artificially Aged (T6) Al-Si-Mg-Based Metal Matrix Composite, *J. Compos. Mater.*, 2006, **40**, p 1259–1269
4. D.B. Miracle and S.L. Donaldson, *ASM Handbook: Composites*, Vol 21, ASM International, Material Park, 2001
5. N. Chawla and K.K. Chawla, *Metal Matrix Composites*, Springer, New York, 2006
6. B. Cantor, F. D, and I. Stone, *Metal and Ceramic Matrix Composites: An Oxford-Kobe Materials Text*, Institute of Physics Publishing, Bristol and Philadelphia, UK, 2004
7. R.S. Mishra, Low Temperature Superplasticity in a Friction-Stir-Processed Ultrafine Grained Al-Zn-Mg-Sc Alloy, *Acta Mater.*, 2005, **53**(15), p 4211–4223
8. C.J. Lee, H.J. C, and P.J. Hsieh, Mg Based Nano-Composites Fabricated by Friction Stir Processing, *Scripta Mater.*, 2006, **54**(7), p 1415–1420
9. D.K. Lim, S. T, and A.P. Gerlich, Synthesis of Multi-Walled CNT Reinforced Aluminium Alloy Composite Via Friction Stir Processing, *Mater. Sci. Eng., A*, 2009, **507**, p 194–199
10. Y. Moruisad, F. H, T. Nagaoka, K. Nogi, and M. Fukusumi, Fullerene/A5083 Composites Fabricated by Material Flow During Friction Stir Processing, *Composites A*, 2007, **38**, p 2097–2101
11. A. Shafiei-Zargani, K.-B.S. F, and A. Zareihanzaki, Microstructures and Mechanical Properties of Al/Al$_2$O$_3$ Surface Nano-Composite Layer Produced by Friction Stir Processing, *Mater. Sci. Eng., A*, 2009, **500**, p 84–91
12. R.S. Mishra, M.M. W, S.X. Mcfadden, N.A. Mara, and A.K. Mukherjee, High Strain Rate Superplasticity in a Friction Stir Processed 7075 Al Alloy, *Scripta Mater.*, 2000, **42**(2), p 163–168
13. J.R. Gomes, A.R. R, A.C. Vieira, A.S. Miranda, and L.A. Rocha, Friction and Wear Properties of Functionally Graded Aluminium Matrix Composites, *Mater. Sci. Forum*, 2003, **425**, p 91–96
14. C.S. Ramesh, A.R.A. K, N. Ravikumar, and P. Savanprabhu, Prediction of Wear Coefficient of Al6061-TiO$_2$ Composites, *Wear*, 2005, **259**, p 602–608
15. J. Hua, D.Y. L, and R. Llewellyn, Computational Investigation of Microstructural Effects on Abrasive Wear of Composite Materials, *Wear*, 2005, **259**, p 6–17
16. J.K.M. Kwok and S.C. L, High-Speed Tribological Properties of Some Al/SiCp Composites: I. Frictional and Wear-Rate Characteristics, *Compos. Sci. Technol.*, 1999, **59**, p 55–63
17. M. Salehi, M. S, and J. Aghazadeh Mohandesi, Optimization of Process Parameters for Producing AA6061/SiC Nanocomposites by

Friction Stir Processing, *Trans. Nonferrous Met. Soc. China*, 2012, **22**, p 1055–1063

18. E. Hornbogen, The Role of Work of Fracture in the Wear of Metals, *Wear*, 1975, **33**, p 251–259

19. I. Sevim, Effect of Work of Fracture on Abrasive Wear Resistance of Steels, *Mater. Des.*, 2006, **27**, p 911–919

20. R.L. Deuis, C. S, and J.M. Yellup, Abrasive Wear of Aluminium Composites—A Review, *Wear*, 1996, **201**, p 132–144

21. S. Amada and S. Untao, Fracture Properties of Bamboo, *Composites B*, 2001, **32**, p 451–459

22. L.L.M. Mishnaevsky, Jr., Functionally Gradient Metal Matrix Composites: Numerical Analysis Of The Microstructure-Strength Relationships, *Compos. Sci. Technol.*, 2006, **66**, p 1873–1887

23. C. Lin, Structure and Properties of Functionally Gradient Aluminium Alloy 2124/SiC Composites, *Mater. Sci. Technol.*, 1994, **10**, p 659–664

24. E. Rabinowicz, *Friction and Wear of Materials*, Wiley, New York, 1995